Preparation of Polyester Nanofibers and Nanofiber Yarns from Polyester/Cellulose Acetate Butyrate Immiscible Polymer Blends

Mufang Li,[1] Ru Xiao,[1] Gang Sun[1,2]

[1]*State Key Lab for Modification of Chemical Fibers and Polymer Materials, College of Materials Science and Engineering, Donghua University, Shanghai 201620, People's Republic of China*
[2]*Department of Fiber and Polymer Science, University of California, Davis, California 95616*

Received 16 April 2010; accepted 23 May 2011
DOI 10.1002/app.34959
Published online 30 September 2011 in Wiley Online Library (wileyonlinelibrary.com).

ABSTRACT: Development of high throughput production processes for making thermoplastic nanofiber and nanofiber yarns are urgently needed. PET, PTT, and PBT nanofibers were prepared from PET/CAB, PTT/CAB, PBT/CAB immiscible polymer blends by *in situ* microfibrillar formation during the melt extruding process. The diameter distribution and crystallization properties of PET, PTT, and PBT nanofibers were analyzed. After removing the CAB matrix phase, the nanofibers could be collected in the forms of random or aligned nanofibers and nanofiber bundles or yarns. To understand the formation mechanism of the nanofibers, the morphology development of three different polyesters in the dispersed phase were studied with samples collected at different zones in a twin-screw extruder. The morphological development mechanism of the dispersed phases involved the formation of sheets, holes and network structures, then the size reduction and formation of nanofibers. © 2011 Wiley Periodicals, Inc. J Appl Polym Sci 124: 28–36, 2012

Key words: blends; nanofibers; nanofiber yarns; phase behavior; polyesters

INTRODUCTION

Because of specific properties of large surface area, good biocompatibility, and low fluid resistance, nanofibers have found applications in many areas, such as improving filtration efficiency of membrane devices, increasing protective and comfort performance of chemical and biological protective clothing, and enhancing the sensitivity of nanosensors.[1] Nanofibers collected in nonwoven forms are acceptable in applications such as composite reinforcements, membrane-based separation, filters, wound dressing and tissue scaffolds, and so forth.[2–6] However, with the development of nanotechnologies, nanofibers are need to be produced in highly ordered structures such as nanofiber bundles or yarns. Well-aligned nanofibers and nanofiber yarns provide an attractive way to process polymeric nanofibers into traditional textiles, which may have applications beyond traditional textiles and can be used in the fields of composites, filtration media, gas separation, sensors, and biomedical engineering.[7–9]

Poly(ethylene terephthalate) (PET), poly(trimethylene terephthalate) (PTT), and poly(butylene terephthalate) (PBT) are three important engineering thermoplastic polyesters, due to their satisfactory mechanical properties. Surface-modified polyester nanofiber materials have found applications in blood vessel engineering, leukocyte removal filters, and tissue scaffolds.[10–13] So far, the developed production methods of nanofibers include electrospinning, melt-blowing, flash spinning, sea-island spinning, and segmented pie bicomponent process.[14–17] By using these methods, PET, PBT, and PTT nanofibers have been prepared successfully.[18–25] However, these methods also have demonstrated issues such as low fiber production efficiency, harsh selection of solvents, and diameter limitation that at certain level restrict their broad applications.

In this study, a newly developed process was used to prepare polyester nanofibers. This method involves choosing two kinds of immiscible thermoplastic polymers, mixing and extruding them from a corotating twin-screw extruder. After removing the matrix phase, nanofibers can be obtained at last.[26–29] The matrix phase of cellulose acetate butyrate (CAB) used in this study is a biobased thermoplastic

Correspondence to: R. Xiao (xiaoru@dhu.edu.cn).
Contract grant sponsor: National Natural Science Foundation of China; contract grant number: 20874010.
Contract grant sponsor: Program of Introducing Talents of Discipline to Universities; contract grant numbers: 111-2-04, B07024.
Contract grant sponsor: Assets Investment Company of Kunshan Development District, Jiangsu Province.

polymer and immiscible with most of other thermoplastics. It could be removed easily with acetone and recycled and reused. Based on this method, PET, PTT, and PBT nanofibers were prepared from PET/CAB, PTT/CAB, PBT/CAB immiscible blends, respectively. The primary focus of the present work was to investigate the formation process of the three different polyesters and morphological development of their nanofibers, which is how the nanofibers formed in the immiscible blends, as well as the properties of the PET, PTT, PBT nanofibers and nanofiber bundles or yarns.

EXPERIMENTAL

Materials

CAB, (CAB-171-15; butyryl content 17 wt %, acetyl content 29.5 wt %, and hydroxyl content 1. 5 wt %, Eastman Chemicals, USA) with a glass transition temperature (T_g) at 161°C and melting point at 230–240°C, was used as a matrix phase. PET was provided by Sinopec Yizheng Chemical Fiber Company (melting point 250–255°C); CORTERRA PTT known as PTT was provided by the Shell Chemicals Europe B.V. (melting point 225–228°C Density1.3–1.44 kg/m^3); PBT was provided by Sinopec Yizheng Chemical Fiber Company with an intrinsic viscosity of 1.30 and melting point at 220–225°C.

Sample preparation

Figure 1 shows the schematic of formation process of nanofibers prepared from the immiscible polymer blends. All of the materials were dried in a vacuum prior to melting and blending. The blends were prepared using a Co-rotating twin-screw extruder (EUROLAB16, D=16mm, L/D=40, Thermo-Haake Co., Germany). The dimension of the extruded die is 4 mm. In the study of the morphology development of the dispersed phase, PET, PTT, and PBT were mixed with CAB at a blend ratio of 20/80 and shear rate of 30 s^{-1}. After extruded from the twin-screw extruder, the size of composite fibers is nearly about 1 mm. Then the composite fibers were immersed in acetone for 24 h, with the solvent changed every 6 h to make sure that the CAB matrix was completely removed.

The screw configuration of the extruder can be seen from Figure 1. Three different sampling points exist in the twin-screw extruder. Different points provide information for the morphologies with different mixing time. The morphology of samples taken from SP-1#, SP-2#, and SP-3# provide information for the initial, metaphase, and later morphological development of the blends, respectively. The melting behavior and morphological development of the blends along the extruder were studied with samples collected at different zones in the extruder. The samples taken from different sampling points were immediately cooled in iced water to preserve the morphology developed in the extruder, and then put into acetone to remove the CAB matrix phase. By these means, the dispersed phase retained the morphology that it exhibited within the blends.

Measurement and characterization

The apparent viscosity of the polymers used in this study was measured using a Capillary Rheometer Instron 4467 (Instron Corp., USA). The elastic modulus of the polymers used in this study was determined by using a dynamical rheometer (ARES-RFS), with a 25-mm parallel plate. The rheological measurements of PET/CAB system were performed at 265°C, while the PTT/CAB and PBT/CAB were performed at 250°C, as the melting points of PET, PTT, PBT are different.

The samples taken from different sampling points and the final nanofibers were observed using a scanning electron microscope (SEM). To observe fracture surfaces of the composite fibers, the composite fibers were fractured in liquid nitrogen and were observed using the SEM.

The crystal properties of PET, PTT, PBT nanofibers after removal of the matrix were investigated by an X-ray diffractometer (XRD, D/max-2550 PC X-Ray Diffractometer, Japan Rigaku Corp.). The X-ray source (Cu Kα radiation, λ = 1.54 E) was generated

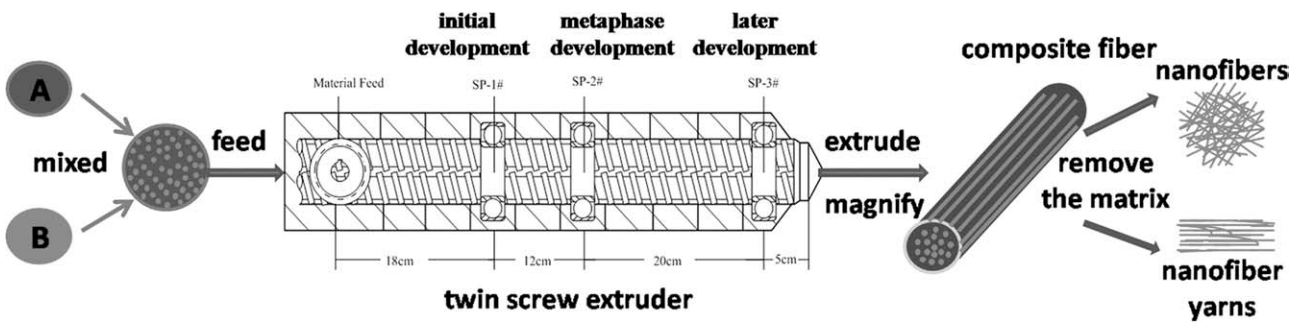

Figure 1 Schematic of formation process of nanofibers prepared from immiscible polymer blends.

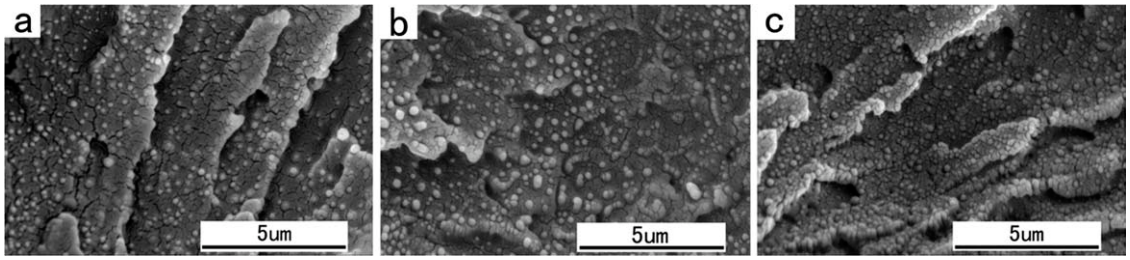

Figure 2 SEM images of fracture surface of polyester/CAB (20/80) (a) PET/CAB, (b) PTT/CAB, (c) PBT/CAB.

using an applied voltage of 40 kV and a filament current of 200 mA.

The diameter distributions and averages were obtained by measuring 100 nanofibers in the SEM viewed areas. The number average diameters were calculated as eq. (1).

$$D_N = \frac{\sum N_i D_i}{\sum N_i} \quad (1)$$

where D_N is the number average diameter, N_i is the number of nanofibers with a diameter of D_i.

RESULTS AND DISCUSSION

Polyester nanofibers

Composite fibers were obtained after the polyester/CAB blends extruded and collected directly from the twin-screw extruder. Figure 2 shows the fracture surfaces of PET/CAB, PTT/CAB, and PBT/CAB composite fibers. It can be seen from Figure 2 that CAB and three kinds of polyester were immiscible completely. The fibrous dispersed phase can be obtained after removing the CAB matrix. As shown in Figure 3, well-defined PET, PTT, and PBT nanofibers were obtained from PET/CAB, PTT/CAB, PBT/CAB immiscible polymer blends after the CAB was removed. What is more, the nanofibers were disordered; this is because the structure of the original nanofibers has been disrupted when we took the SEM samples. Figure 4 shows the diameter distribution of PET, PTT, and PBT nanofibers. It can be seen that the diameter distributions of three polyester nanofibers were quite uniform, ranging in 50–300 nm. The average diameters of PET, PTT, and PBT nanofiber were 179, 145, 137 nm, respectively. The diameters of polyester nanofibers obtained by this method are smaller than those via electrospinning.[19–24]

PET, PTT, and PBT are linear aromatic polyesters. The X-ray diffraction patterns for PET, PTT, and PBT nanofibers are shown in Figure 5. It can be seen from Figure 5 that, the PET nanofibers obtained from the PET/CAB immiscible blends showed peaks at the scattering angles 2θ of 16.7, 17.7, 22.9, 25.8, and 32.5, corresponding to (0 $\bar{1}$ 1), (0 1 0), (1 $\bar{1}$ 0), (1 0 0), and (1 0 1) scattering planes of PET, respectively. The characteristic X-ray peaks of PTT nanofibers were observed at the scattering angles 2θ of 15.6, 16.7, 19.9, 21.8, 23.5, 24.5, and 27.2, corresponding to the reflection planes of (0 1 0), (0 $\bar{1}$ 2), (0 1 2), (1 0 $\bar{2}$), (1 0 2), (1 1 $\bar{3}$), and (1 0 $\bar{4}$), respectively. The PBT nanofibers showed peaks at the scattering angles 2θ of 15.7, 17.0, 19.9, 23.3, 24.8, and 31.0, corresponding to the (0 $\bar{1}$ 1), (0 1 0), (0 1 1), (1 0 0), (1 $\bar{1}$ 1), and ($\bar{1}$ 0 4), respectively.[30,31] Three different polyester nanofibers all exhibited the same diffraction peaks to their neat polyester fibers. High deformation and elongation could cause high orientation of polymer chains in the fibers; thus the crystallinity and orientation of PET, PTT, and PBT nanofibers could be affected by the mixed process.

Collection of nanofibers or yarns

Polyester nanofibers can be obtained by immersing the coarse composite fibers in acetone and removing the matrix. As the nanofibers formed in this study are an untwisted group of a large number of short nanofibers with uniaxial alignment, if keeping

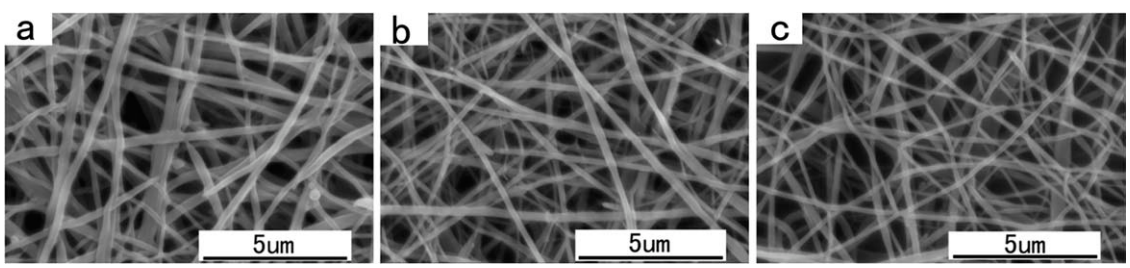

Figure 3 SEM images of polyester nanofibers prepared from polyester/CAB (20/80) blends (a) PET, (b) PTT, (c) PBT.

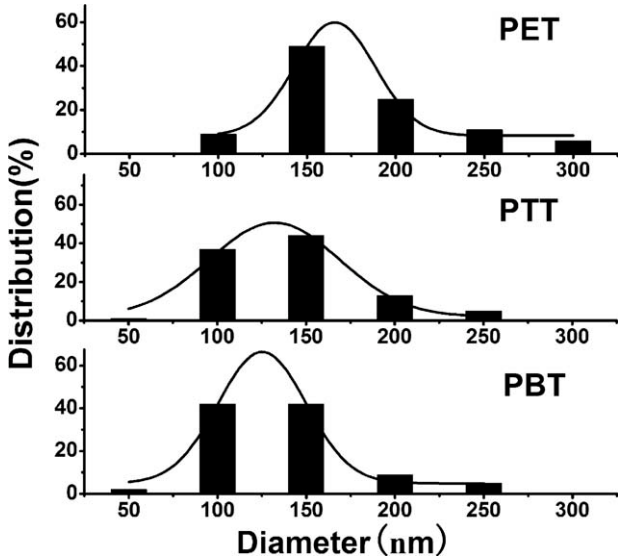

Figure 4 Diameter distribution of PET, PTT, and PBT nanofibers obtained from polyester/CAB (20/80) blends after extruding from the extruder, with the same draw ratio.

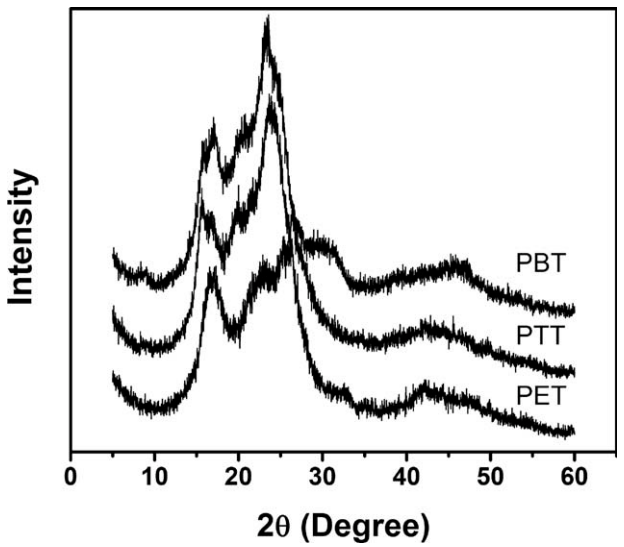

Figure 5 XRD patterns for PET, PTT, and PBT nanofibers prepared from PET/CAB, PTT/CAB, PBT/CAB (20/80) blends, with the same processing conditions.

the original morphology of the filament, the nanofibers could retain in the form of bundles or yarns. Figure 6(a) shows the morphology of the remaining PTT nanofiber bundles or yarns that were immersed in acetone. Figure 6(b) shows the morphology of nanofiber bundles or yarns after taking out from the acetone. The form of nanofiber yarns or bundles makes it controllable for further processing into desired shapes and patterns. Just as shown in Figure 6(b), the as-prepared PTT nanofiber bundles or yarns could then be knitted and braided manually to fabricate mesh fabric and

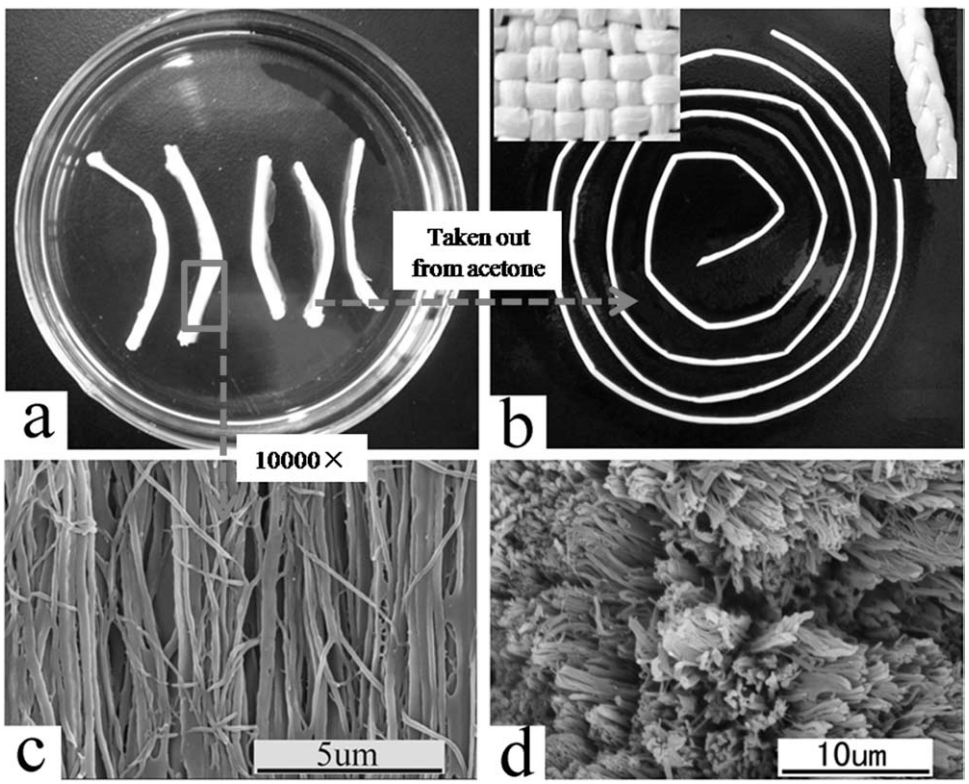

Figure 6 Preparation and morphology of PTT nannofiber yarns (a) Photograph of orderly nanofibers immersing in acetone, (b) photograph of nanofiber yarns after taking out from acetone, (c) SEM image of surface morphology of nanofiber yarns, (d) SEM image of fracture surface of nanofiber yarns.

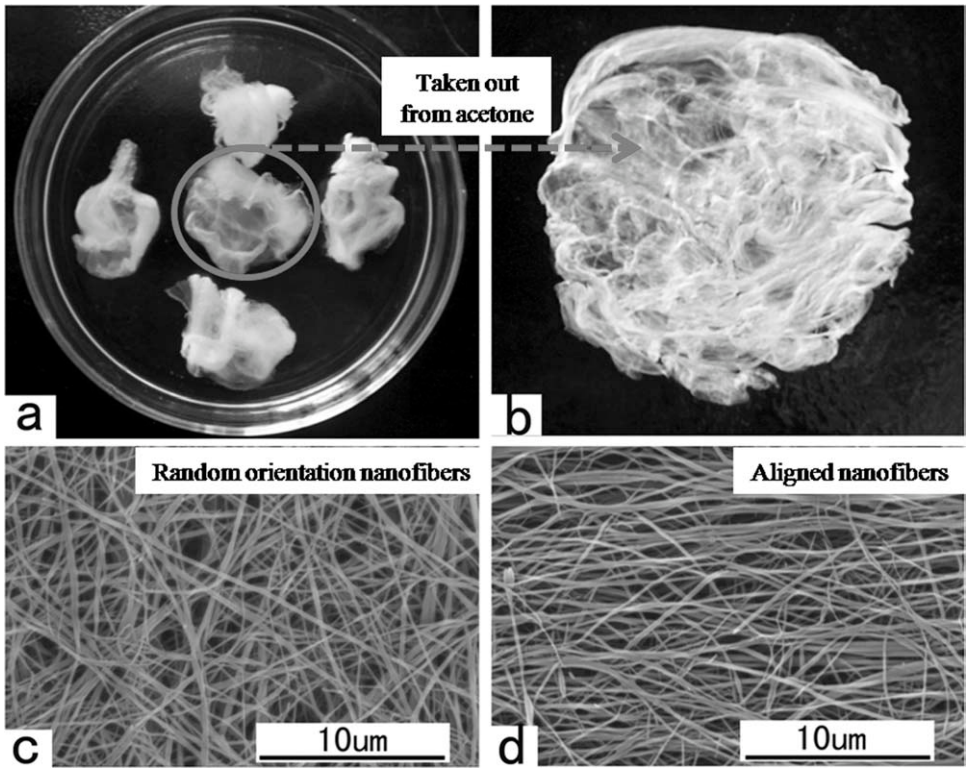

Figure 7 Collection of PTT nanofibers from PTT/CAB composite fibers (a) Photograph of disordered nanofibers immersing in acetone, (b) photograph of nanofibers after taking out from acetone, (c) SEM image of random orientation nanofibers, (d) SEM image of aligned nanofibers.

rope. The inner structures and the alignment play key roles in the properties of the nanofiber bundles or yarns. Figure 6(c,d) reveal the surface and fracture surface morphologies of nanofiber bundles or yarns. It can be seen from Figure 6(c) that the nanofiber yarns in this study are an untwisted group of a large number of short nanofibers with uniaxial alignment.

However, the CAB matrix is difficult to be removed clearly if keeping the original structure of the nanofibers. Therefore, the original structure of nanofiber yarns should be disrupted in normal conditions, then the nanofibers would be disordered and exist in acetone in disordered form such as cotton fibers in water, as shown in Figure 7(a). Figure 7(b) shows the morphology of nanofibers after taking out

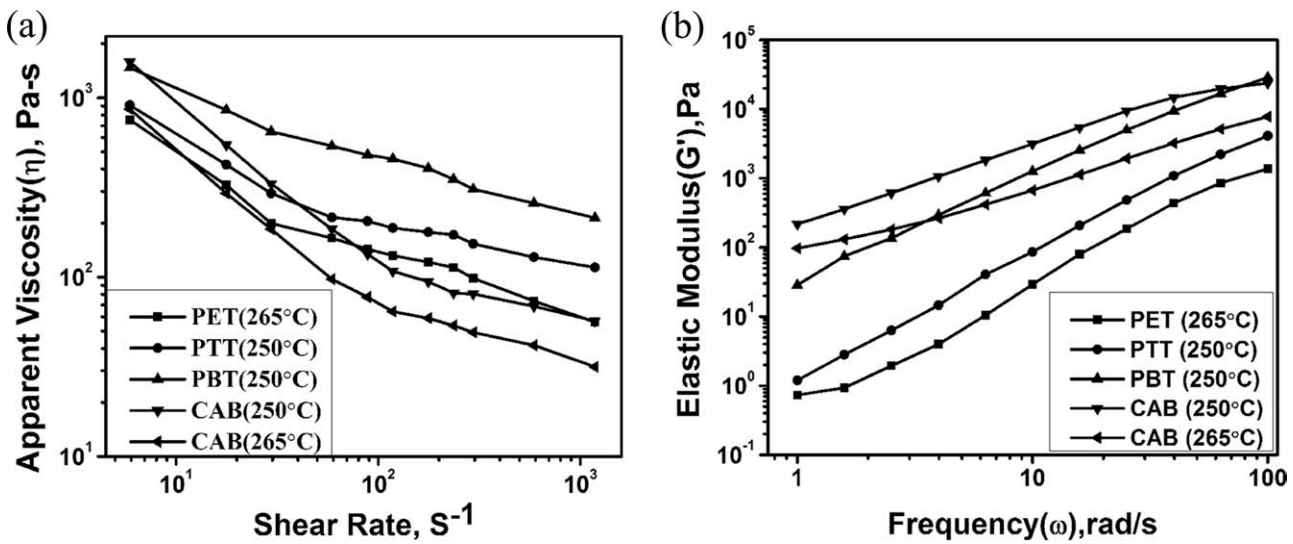

Figure 8 (a) Apparent viscosity and (b) elastic modulus for all polymers as a function of shear rate and frequency.

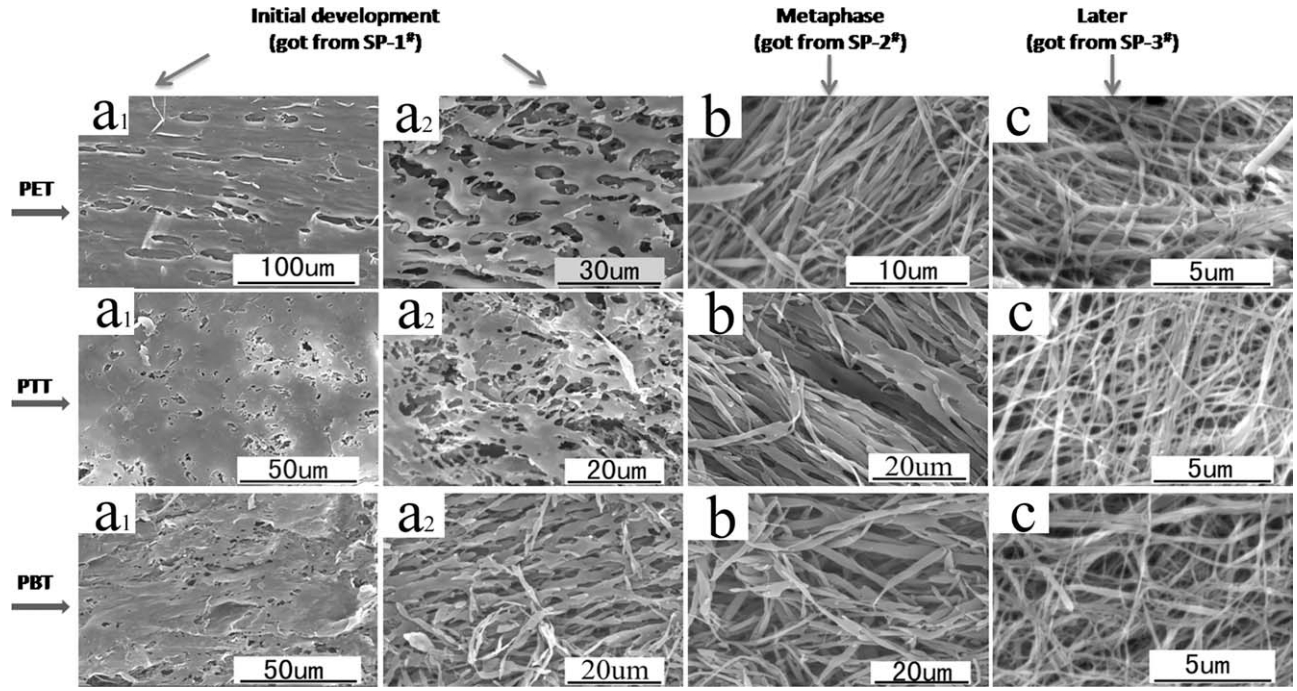

Figure 9 Morphological development of PET, PTT, and PBT nanofibers prepared from polyester/CAB immiscible blends, at the same blend ratio of polyester/CAB = 20/80, and the same shear rate (30 s^{-1}).

from acetone. Normally, the nanofibers become randomly oriented, as shown in Figure 7(c). However, as shown in Figure 7(d), the nanofibers could be aligned using external forces. If using a suitable carding machine, the nanofibers could be carded just like wool or cotton fibers.

Analysis of the formation of nanofibers

The formation of PET, PTT, and PBT nanosized fibers in the twin-screw extruder was an overall result of continuous deformation, elongation, orientation, and coalescence of dispersed micelles to nanofibers in CAB matrix. The conditions for fibril formation were very complicated, viscosity ratio (η_d/η_m, η_d is the viscosity of the dispersed phase, η_m is the viscosity of the matrix phase) played an important role on the deformation of the dispersed phase.[27] The effect of viscosity ratio (η_d/η_m) on the fibril formation of different polymer blends has been analyzed in detail.[32] Fibrils could form at a viscosity ratio range of $0.3 < \eta_d/\eta_m < 1.0$ for polyethylene/polystyrene blends, $\eta_d/\eta_m > 3.7$ for PET/polyamide blends, and $\eta_d/\eta_m < 1$ for polypropylene/ethylene-propylene copolymer blends.[32] He et al. and Plate et al. studied 13 different pairs of polymers and indicated that good fibrillation can be achieved when the viscosity ratio was in the range of $0.1 < \eta_d/\eta_m < 10$.[33,34]

For studying the rheological properties of all the materials used in this study, the apparent viscosity (η) as a function of shear rate, with PET, CAB at 265°C and PTT, PBT, CAB at 250°C, are shown in Figure 8(a). The dynamic elastic moduli (G′) of the polymers are plotted versus frequencies shown in Figure 8(b). With increasing of the shear rate, the apparent viscosity decreased continuously, implying that the PET, PTT, PBT, and CAB were non-Newtonian fluids and all followed the shear thinning behavior. For the system of PET/CAB, PTT/CAB, PBT/CAB, at the shear rate of 30 s^{-1}, the viscosity ratio is 1.1, 0.9, 2.0, respectively. Therefore, fibrillar dispersed phase can be obtained after removing the matrix phase.

The dispersed phase of PET, PTT, and PBT were added at room temperature as pellets, while the matrix phase of CAB was added as powder. When the mixed materials were fed into the twin-screw extruder, a serious deformation will happen,[35] making the dispersed phase transformed from pellets to the final nanosized fibers. Figure 9 shows the morphology development of PET, PTT, and PBT dispersed phase after the polymer blends were taken from different sampling points in the extruder and removing the matrix. As the melting of the polymer blends was a multistage process, the morphologies of the PBT dispersed phase were very complex in the initial stage of compounding. Two different representative SEM images were chosen for each sample, as shown in Figure 9(a_1,a_2), to describe the mechanism of the initial morphological development. Figure 9(b,c) displayed the morphology of metaphase and later phase development.

TABLE I
Average Diameters and Standard Deviation (SD) of Polyester Nanofibers Obtained at Different Processing Conditions, with the Same Blend Ratio of Polyester/CAB = 20/80 and the Same Shear Rate 30 s^{-1}

Samples	Viscosity raito (η_d/η_m)	Average diameter and SD from SP-2# (nm)	Average diameter and SD from SP-3# (nm)	Average diameter and SD after extrusion (nm)
PET	1.1	355 (12.19%)	155 (4.39%)	179 (4.83%)
PTT	0.9	737 (16.95%)	109 (2.77%)	145 (4.06%)
PBT	2.0	819 (24.38%)	105 (2.61%)	137 (3.98%)

The initial morphological development of PET, PTT, and PBT shows remarkably similar types of structures. The quick morphological changes in the initial stage of blending are caused by the "sheeting" mechanism.[36,37] This mechanism involves the formation of sheets or ribbons when a large piece of dispersed phase was dragged across the hot surface, as shown in Figure 9(a_1). As a result of the effect of shear flow and interfacial tension, the sheets were unstable and began to break down resulting in formation of holes in them; the holes were filled with the matrix phase. When the holes attained sufficient size and concentration, they would coalesce and form network structures, as shown in Figure 9(a_2). Therefore, the initial morphology development procedure for the dispersed phase of polyester in the matrix was from pellets to sheets or ribbons, and then the sheets or ribbons formed holes and network structures.

Figure 9(b) shows the metaphase development of the PET, PTT, PBT dispersed phase. It can be seen that microfibers began to form at SP-2#, as an enormous reduction in phase size taking place from SP-1# to SP-2#. It has been proved that several different morphologies existed in the samples taken from SP-1#, as the melting of PBT dispersed pellets was a multistage process. At SP-2#, however, most of samples were fibers, because the materials have melted and deformed mostly, massive fibers formed by breaking up of the network structures. Therefore, the metaphase development of the olyester dispersed phase can be described as the formation of fibers.

Figure 9(c) displays the later morphological development of the PET, PTT, and PBT dispersed phase. It can be seen that nanofibers were further developed in the later stage. Table I lists the average diameters of PET, PTT, and PBT nanofibers obtained from different processing stages. Comparing the fibers taken from SP-2# with those taken from SP-3#, the fibers obtained from SP-3# were smaller than those taken from SP-2#, respectively. The decline of average diameter from SP-2# to SP-3# indicates that the later morphological development of the polyester dispersed phase is a reduction in diameter of the fibers. Figure 9 also reveals that the holistic developmental trends of PET, PTT, and PBT are nearly the same. Then, the whole formation process of nanofibers can be confirmed and the Schematic diagram given below, shown in Figure 10.

Previous researches have demonstrated that most of the particle size reduction occurred in conjunction with the melting and softening processes, where an enormous reduction in phase size took place.[38] Once the melting was completed, only minor changes took place. This phenomenon was also observed in this study. In the initial and metaphase development of the polymer blends, the mechanism of the deformation of sheets followed

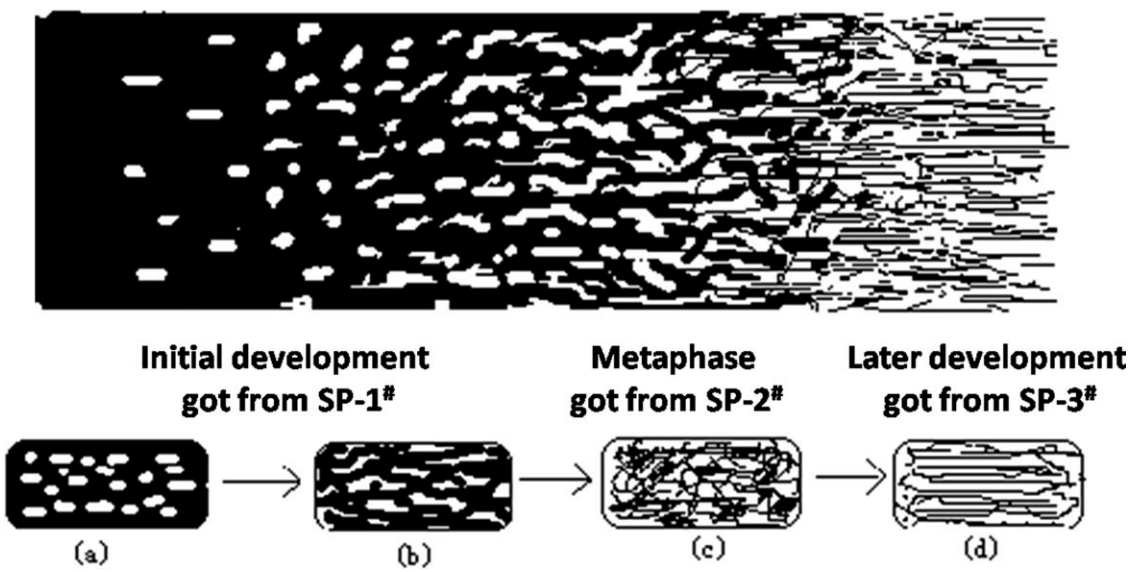

Figure 10 Schematic diagram of morphology development of the dispersed phase.

by a break-up and formation of fibers was an effective way to rapidly decrease the original diameter of the dispersed phase. In the later development of the blends, however, under the effects of elongation effect caused by the shear flow field, a further reduction in diameter of fibers took place between SP-2# to SP-3#. Though this reduction was unconspicuous, it is pivotal for the formation of the final nanofibers. However, as shown in Table I, comparing the samples taken from SP-3# with those after extrusion, the average diameters of PET, PTT, and PBT nanofibers become larger after the polymer blends were extruded. Perhaps it is because that the interference and coalescence of the dispersed phase increased when it flows through the exit of the die and undergoes the elongation flow field.

As the processing parameters used in this study are unchangeable, the size distribution of three kinds of polyester nanofibers mainly affected by the diversity of materials properties, as shown in Table I. It is well known that in a polymer–polymer blend, both viscosity and elasticity play important roles in the droplet break-up process, higher viscosity and elasticity of the dispersed phase will resist the breaking up of droplet.[39,40] As can be seen from Figure 8, the average diameter of PET in the SP-2# was the smallest. It is because that the materials were not melted and deformed completely at this period. From SP-1# to SP-2#, there is a transformative process of the dispersed phase from pellets to sheets, holes, and network structures. As the viscosity and elastic modulus of PET is the smallest, its transformation of the dispersed phase will be easier than PTT and PBT. Therefore, the average diameter of PET in the SP-2# was the smallest.

However, for the samples taken from the SP-3# and after extrusion, the average diameter of PET nanofibers was the largest. It is because that the materials were melted and deformed completely at this period, massive fibers formed by breaking up of the network structures. On the one hand, the number average diameter increased with viscosity ratio, as high viscosity ratios hamper the droplet break-up process.[41,42] Moreover, much larger droplets were formed at low viscosity ratio due to low length stretching.[43] In this study, though η_d/η_m (PTT/CAB) $<$ η_d/η_m (PET/CAB) $<$ η_d/η_m (PBT/CAB), the average diameter of PET nanofibers is the largest. It is difficult to conclude the direct relationship between viscosity ratio and the size distribution of nanofibers. Therefore, in consideration of multifactor effect, the diameter variation for PET nanofiber may attribute to multiple break-up patterns, the interference of neighboring fibrils and the elasticity, coalescence of the dispersed phase.[44]

CONCLUSION

Well-defined PET, PTT, and PBT nanofibers were prepared from PET/CAB, PTT/CAB, PBT/CAB immiscible blends. The average diameters of the obtained PET, PTT, and PBT nanofibers are nearly 200 nm. The nanofibers prepared by this method can be collected in the forms of random and aligned orientation. Continuous nanofiber bundles or yarns can be obtained if the original morphology of the filament retained. The morphology developmental trends of PET, PTT, and PBT dispersed phase, from initial to metaphase and later phase development, are nearly the same. The initial morphology development process for the dispersed phase was the formation of pellets to sheets or ribbons, and then dispersed network structures. The metaphase development of the dispersed phase could possibly explain the formation of fibers. The later phase development of the dispersed phase mainly involved the reduction in diameter of the fibers to the nanoscale.

References

1. Reneker, D. H.; Chun, I. Nanotechnology 1996, 7, 216.
2. Yoon, K.; Hsiao, B. S.; Chu, B. Polymer 2009, 50, 2893.
3. Ma, Z. W.; Lan, Z. W.; Matsuura, T.; Ramakrishna, S. J Chromatogr B 2009, 877, 3686.
4. Lee, J. J.; Yu, H. S.; Hong, S. J.; Jeong, I.; Jang, J. H.; Kim, H. W. J Mater Sci Mater Med 2009, 20, 1927.
5. Kim, G. H.; Yoon, H. Appl Phys A 2008, 90, 389.
6. Feng, C.; Khulbe, K. C.; Matsuura, I.; Gopal, R.; Kaur, S.; Rarnakrishna, S.; Khayet, A. J Membr Sci 2008, 311, 1.
7. Sarkar, S.; Deevi, S.; Tepper, G. Macromol Rapid Commun 2007, 28, 1034.
8. Xu, C. Y.; Inai, R.; Kotaki, M.; Ramakrishna, S. Biomaterials 2004, 25, 877.
9. Yao, C.; Li, X. S.; Song, T. Y. J Appl Polym Sci 2009, 114, 2079.
10. Veleirinho, B.; Lopes-da-Silva, J. A. Proc Biochem 2009, 44, 353.
11. Kim, E. J.; Yeo, G. D.; Pai, C. M.; Kang, I. K. J Biomed Mater Res B 2009, 90, 849.
12. Zhang, W. Y.; Yi, X. P.; Sun, X. M.; Zhang, Y. X. J Chem Technol Biotechnol 2008, 83, 904.
13. Ma, Z. W.; Kotaki, M.; Yong, T.; He, W.; Ramakrishna, S. Biomaterials 2005, 26, 2527.
14. Zhou, F. L.; Gong, R. H. Polym Int 2008, 57, 837.
15. Agarwal, S.; Greiner, A.; Wendorff, J. H. Adv Funct Mater 2009, 19, 2863.
16. Dalton, P. D.; Klinkhammer, K.; Salber, J.; Klee, D.; Moller, M. Biomacromolecules 2006, 7, 686.
17. Ellison, C. J.; Phatak, A.; Giles, D. W.; Macosko, C. W.; Bates, F. S. Polymer 2007, 48, 3306.
18. Suzuki, A.; Tanizawa, K. Polymer 2009, 50, 913.
19. Veleirinho, B.; Rei, M. F.; Lopes-da-Silva, J. A. J Polym Sci Part B: Polym Phys 2008, 46, 460.
20. Jung, K. H.; Huh, M. W.; Meng, W.; Yuan, J.; Hyun, S. H.; Bae, J. S.; Hudson, S. M.; Kang, I. K. J Appl Polym Sci 2007, 105, 2816.
21. Mathew, G.; Hong, J. P.; Rhee, J. M.; Leo, D. J.; Nah, C. J Appl Polym Sci 2006, 101, 2017.
22. Mathew, G.; Hong, J. P.; Rhee, J. M.; Lee, H. S.; Nah, C. Polym Test 2005, 24, 712.
23. Kim, K. W.; Lee, K. H.; Khil, M. S.; Ho, Y. S.; Kim, H. Y. Fiber Polym 2004, 5, 122.

24. Khil, M. S.; Kim, H. Y.; Kim, M. S.; Park, S. Y.; Lee, D. R. Polymer 2004, 45, 295.
25. Nakata, K.; Fujii, K.; Ohkoshi, Y.; Gotoh, Y.; Nagura, M.; Numata, M.; Kamiyama, M. Macromol Rapid Commun 2007, 28, 792.
26. Wang, D.; Sun, G. Eur Polym Mater 2007, 43, 3587.
27. Wang, D.; Sun, G.; Chiou, B. S. Macromol Mater Eng 2007, 292, 407.
28. Wang, D.; Sun, G.; Chiou, B. S. Macromol Mater Eng 2008, 293, 657.
29. Wang, D.; Sun, G.; Chiou, B. S.; Hinestroza, J. P. Polym Eng Sci 2007, 47, 1865.
30. Dangseeyun, N.; Supaphol, P.; Nithitanakul, M. Polym Test 2004, 23, 187.
31. Wang, Z. G.; Hsiao, B. S.; Fu, B. X.; Liu, L.; Yeh, F.; Sauer, B. B.; Chang, H.; Schultz, J. M. Polymer 2000, 41, 1791.
32. Kim, B. K.; Do, I. H. J Appl Polym Sci 1996, 60, 2207.
33. He, J. S.; Bu, W. S.; Zhang, H. Z. Polym Eng Sci 1995, 35, 1695.
34. Plate, N. A.; Kulichikhin, V. G.; Talroze, R. V. Pure Appl Chem 1991, 63, 925.
35. Lin, B.; Sundararaj, U.; Mighri, F.; Huneault, M. A. Polym Eng Sci 2003, 43, 891.
36. Lee, J. K.; Han, C. D. Polymer 1999, 40, 6277.
37. Scott, C. E.; Macosko, C. W. Polymer 1995, 36, 461.
38. Bawiskar, S.; White, J. L. Int Polym Proc 1995, 10, 105.
39. Wallheinke, K.; Potschke, P.; Stutz, H. J Appl Polym Sci 1997, 65, 2217.
40. Ghodgaonkar, P. G.; Sundararaj, U. Polym Eng Sci 1996, 36, 1656.
41. Serpe, G.; Jarrin, J.; Dawans, F. Polym Eng Sci 1990, 30, 553.
42. Everaert, V.; Aerts, L.; Groeninckx, G. Polymer 1999, 40, 6627.
43. Tjahjadi, M.; Ottino, J. M. J Fluid Mech 1991, 232, 191.
44. Jana, S. C.; San, M. Polymer 2004, 45, 1665.